

# Modeling of the N<sub>2</sub>O<sub>4</sub>–NO<sub>2</sub> reacting system

Luís E. S. de Souza and Ulrich K. Deiters\*

Institut für Physikalische Chemie, Universität zu Köln, Luxemburger Strasse 116,  
D-50939 Germany

Received 7th July 2000, Accepted 24th October 2000

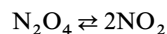
First published as an Advance Article on the web 23rd November 2000

Reaction systems containing the nitrogen oxides N<sub>2</sub>O<sub>4</sub> and NO<sub>2</sub> in equilibrium, pure or dissolved in organic solvents, are successfully modeled in two ways: (1) assuming that all species in the system are hard spheres with an attractive mean field component (HSA); and (2) using a semiempirical equation of state (EOS) developed by Deiters. In both cases, estimates of the relative size of the species, obtained by Monte Carlo (MC) simulations, were made to reduce the number of adjustable parameters. As a result, for a pure system, both the HSA model and the semiempirical EOS require only three adjustable parameters. MC simulations were also employed to estimate semiempirical EOS anisotropy parameters for each species without a need of experimental data. In this way, the truly adjustable parameters were obtained by taking only experimental data for the system at 296 K. The agreement between both model predictions and experimental results is good, with higher accuracy for the semiempirical EOS. The predicted effect of pressure on the equilibrium constant of the gas mixture is underestimated by both models. For the case of the nitrogen oxides dissolved in a third species, the HSA model and the semiempirical EOS require two and three additional parameters respectively, which are determined from experimental data of the neat solvent in the liquid–vapor coexistence region. Calculations were performed for CCl<sub>4</sub> and cyclohexane as solvents. The predicted dissociation constants of N<sub>2</sub>O<sub>4</sub> in the liquid phase are underestimated by about 25% by the HSA model and overestimated by 5% by the semiempirical EOS.

## 1 Introduction

Several equations of state (EOS) and other analytical models for the determination of thermodynamical properties of mixtures have been developed in recent decades. The aim of this effort is not only to be able to fit experimental data, but also to use those approaches as tools for interpolation and prediction. In this context, formulations which involve a small number of parameters have the advantage of requiring few experimental measurements in the fitting procedure. In industry, experimental measurements are often costly and therefore avoided whenever possible. Unfortunately, accurate models often require several adjustable parameters and are usually not reliable outside the region where the experimental data were taken from.

In this work, two equations of state are shown to be useful for fitting and predicting the thermodynamic properties of a reacting system. The system of choice is N<sub>2</sub>O<sub>4</sub>–NO<sub>2</sub> for a number of reasons. First, it is relatively simple, *i.e.*, both NO<sub>2</sub> and N<sub>2</sub>O<sub>4</sub> are rigid molecules with few atoms. Secondly, the chemical equilibrium



is achieved very quickly, which has allowed the experimental measurement of equilibrium constants, phase behavior and pressure–volume–temperature (*pVT*) dependence. The relative richness of experimental data allows the testing of molecular size and shape effects, as well as those effects that arise from the relatively complex attractive pair potentials. Some experimentally measured dissociation constants of N<sub>2</sub>O<sub>4</sub> in cyclohexane and CCl<sub>4</sub> can also be used to test the ability of the equations of state to predict without any specific input data for the three-species mixture. Finally, equilibrium constant

measurements above room temperature are scarce and incomplete. Because of this, predictions of unmeasured properties of the system can also be drawn from the two equations of state.

The first model considered in this work, referred to as HSA, requires only the knowledge of the thermodynamic reaction parameters in the perfect gas state and a few experimental data points. The molecules are modeled as hard spheres (HS) with a mean field-type attraction. Dissociation reactions have already been studied with a similar approach by de Souza and Ben-Amotz.<sup>1</sup> In their work, calculations were performed for the dissociation of a fused hard sphere in a hard-sphere fluid, yielding two hard spheres. All species in the system also had mean field attractive parameters associated with them. In contrast, the present HSA model treats all species (including the pseudo-diatomic N<sub>2</sub>O<sub>4</sub>) as spheres. The dissociation of bromine in rare gases has also been studied theoretically by a Lennard-Jones perturbed HS model.<sup>2</sup>

The second equation of state considered here, which is expected to be more accurate, was developed by Deiters<sup>3–5</sup> and will be referred to hereafter as the semiempirical equation of state, SES. Such an equation has been applied to a variety of fluid mixtures with good results and requires an additional parameter for each species, associated with shape. In this paper, we investigate the possible improvement which can be obtained with such accurate EOS.

This work is divided into five sections. This introduction is followed by a theoretical section, where the main assumptions and features of the HSA and SES formulations are presented. Section 3 describes the determination of parameters for the N<sub>2</sub>O<sub>4</sub>–NO<sub>2</sub> system required by such models. Section 4 contains the results of this work, which are compared with experimental data. Finally, in Section 5 the results are discussed and conclusions are presented.

## 2 Theoretical formulation

### 2.1 Equilibrium requirements

In a one-phase system composed of  $N_2O_4$ ,  $NO_2$  and a solvent (denoted as species 1, 2 and 3 respectively) at a temperature  $T$ , chemical equilibrium requires

$$\mu_1 = 2\mu_2 \quad (1)$$

where  $\mu_i$  is the chemical potential of species  $i$ . In a two-phase system, eqn. (1) is valid for both the liquid and vapor phases. However, the decrease in degrees of freedom of the system introduces additional constraints: the chemical potential of any species in the liquid phase ( $\mu_i^L$ ) needs to be equal to that in the vapor phase ( $\mu_i^V$ ) and the pressure in the liquid phase ( $p_L$ ) must be equal to that in the vapor phase ( $p_V$ ). For the  $N_2O_4$ – $NO_2$  system, the requirements above are sufficient to determine the phase diagram, and also the system density and composition as a function of pressure and temperature. In the presence of a third species (solvent), additional information, such as the mass ratio of the nitrogen oxides ( $NO_2$  and  $N_2O_4$ ) to solvent in a given phase, is needed.

The calculations require expressions for the chemical potentials of each species in each phase and for the pressure. Such expressions are derived below for the HSA and SES formulations.

### 2.2 The HSA model and its basic expressions

The configuration integral,  $Z_N$ , for the system, composed of  $N$  species ( $n_1$  moles of  $N_2O_4$ ,  $n_2$  moles of  $NO_2$  and  $n_3$  moles of solvent) at a volume  $V$  and temperature  $T$  is assumed in the HSA model to be

$$\begin{aligned} Z_N &= Z_N^{\text{HS}} \exp\{[(n_1 + n_2 + n_3)a\rho]/kT\} \\ &= Z_N^{\text{HS}} \exp\{(na\rho)/kT\} \end{aligned} \quad (2)$$

where  $k$  is Boltzmann's constant,  $\rho = n/V$ , and  $a$  is a function of the mole fractions of all species in the system,  $\mathbf{x} = \{x_1, x_2, x_3\}$ . The attractive parameters for the interaction between each pair of species  $i$  and  $j$ ,  $a_{ij}$ , are given by

$$a = \frac{1}{2} \sum_{i=1}^3 x_i \sum_{j=1}^3 x_j a_{ij} \quad (3)$$

where

$$a_{ij} = (a_{ii}a_{jj})^{1/2} \quad (4)$$

The quantity  $Z_N^{\text{HS}}$  is the configuration integral of a HS system with same composition, density and temperature as the real system, and composed of hard spheres of diameters  $d_1$ ,  $d_2$  and  $d_3$ . The properties of such a hard sphere reference system are taken to be those described by Mansoori *et al.*<sup>6</sup>

With the definitions above, the Helmholtz free energy of a given phase of volume  $V$  and at a temperature  $T$  can be divided into two parts, a non-interacting term (ideal) and a residual, interacting term:

$$\begin{aligned} A(n, \mathbf{x}, V, T) &= [A^{\text{id}}(n_1, V, T) + A^{\text{id}}(n_2, V, T) \\ &\quad + A^{\text{id}}(n_3, V, T)] + A^{\text{res}}(n, \mathbf{x}, V, T) \end{aligned} \quad (5)$$

The residual part of the Helmholtz free energy contains a HS and an attractive term,

$$\begin{aligned} A^{\text{res}}(n, \mathbf{x}, V, T) &= -kT \ln(Z_N/V^N) \\ &= -kT \ln(Z_N^{\text{HS}}/V^N) - na\rho \\ &= A^{\text{HS}}(n, \mathbf{x}, V, T) - na\rho \end{aligned} \quad (6)$$

where<sup>6</sup>

$$\begin{aligned} \frac{A^{\text{HS}}(n, \mathbf{x}, V, T)}{nRT} &= \frac{3y_2 + 2y_3}{1 - \eta} \\ &\quad + \frac{3}{2} \frac{1 - y_1 - y_2 - y_3/3}{(1 - \eta)^2} \\ &\quad - \frac{3}{2}(1 - y_1 + y_2 + y_3) + (y_3 - 1)\ln(1 - \eta) \end{aligned} \quad (7)$$

In eqn. (7),  $R$  is the molar gas constant, and the packing fraction  $\eta$  and  $y_1, y_2, y_3$  are defined by<sup>6</sup>

$$\eta = \sum_{i=1}^3 \eta_i = \sum_{i=1}^3 \frac{\pi N}{6V} x_i d_i^3 \quad (8)$$

$$y_1 = \sum_{j>i=1}^3 A_{ij}(d_i + d_j)(d_i d_j)^{-1/2} \quad (9)$$

$$y_2 = \sum_{j>i=1}^3 A_{ij} \sum_{k=1}^3 \left(\frac{\eta_k}{\eta}\right) \frac{(d_i d_j)^{1/2}}{d_k} \quad (10)$$

$$y_3 = \left[ \sum_{i=1}^3 \left(\frac{\eta_i}{\eta}\right)^{2/3} x_i^{1/3} \right]^3 \quad (11)$$

with

$$A_{ij} = [(\eta_i \eta_j)^{1/2}/\eta][(d_i - d_j)^2/d_i d_j](x_i x_j)^{1/2} \quad (12)$$

Using eqns. (5) and (6), the pressure and the chemical potential of each species  $i$  can be calculated by taking the appropriate derivatives of the Helmholtz free energy and using the fact that

$$\left[ \frac{\partial A^{\text{id}}(n_i, V, T)}{\partial n} \right]_{V, T} = \mu_i^{\text{id}} = \mu_i^{\text{id}}(p^\circ, T) + RT \ln \left[ \frac{x_i \rho RT}{p^\circ} \right] \quad (13)$$

where  $p^\circ$  is a reference pressure.

### 2.3 The semiempirical equation of state (SES)

The second formulation used in this work to model the  $N_2O_4$ – $NO_2$  system was developed by Deiters.<sup>3–5</sup> The properties of a fluid mixture are described in terms of the properties of a pure reference fluid with three adjustable parameters,  $T^*$ ,  $b$  and  $c$ , where  $T^*$  is an attractive parameter, usually expressed in kelvin,  $b$  is a measure of the molecule size in the reference fluid (usually expressed in  $\text{cm}^3 \text{mol}^{-1}$ ), and the parameter  $c$ , related to the molecule's anisotropy, is dimensionless. The residual part of the Helmholtz free energy can be expressed as<sup>5</sup>

$$A^{\text{res}} = cc_0 A^{\text{HS}} - \frac{nRT^* \rho}{c^2} [h_0 \gamma^2 \psi(\tilde{T}) + F_1] \quad (14)$$

where  $h_0 = 7.0794046$ ,  $a_0 = 0.6887$ ,  $\rho = b/V_m$  and<sup>3</sup>

$$\tilde{T} = \frac{cT}{T^*} \quad (15)$$

$$\psi(\tilde{T}) = \tilde{T} [\exp(\tilde{T}^{-1}) - 1] \quad (16)$$

$$\gamma = 1 - 0.697816(c - 1)^2 \quad (17)$$

The function  $F_1$  in eqn. (14) is defined elsewhere.<sup>5</sup> The quantity  $A^{\text{HS}}$  represents the Helmholtz free energy of a hard sphere system. Originally,<sup>3–5</sup> such a reference system was assumed to be that of a neat HS system. In this work, we chose that of a mixture of hard spheres, as described by Mansoori *et al.*<sup>6</sup> and used in the HSA model, according to eqns. (7) to (12). Although this refinement did not significantly improve the accuracy of the results, it facilitates the comparison between the performance of the HSA model and eqn. (14). Combining eqn. (14) with eqn. (13), the pressure and chemical potentials can be calculated as in the HSA model case.

Eqn. (14) can normally be applied both to a pure fluid and to a mixture, but in the latter case the parameters  $T^*$  and  $c$  for the reference pure fluid are obtained from the corresponding parameters for each of the species  $i$  in the mixture ( $T_i^*$  and

$c_i$ ) and the system composition. The mixing rules adopted in this work are as follows. For the parameter  $c$ ,<sup>5</sup>

$$c = \sum x_i c_i \quad (18)$$

For the parameter  $T^*$ ,<sup>7</sup>

$$T^* = (\sum x_i \sum x_k T_{ik}^* b_{ik}^{7/3}) / (\sum x_i \sum x_k b_{ik}^{7/3}) \quad (19)$$

where

$$T_{ik}^* = (T_i^* T_k^*)^{1/2} \quad (20)$$

$$\gamma = 3(1 - \xi^2) \quad (21)$$

$$b_{ik} = (b_i + b_k)/2 \quad (22)$$

An alternative for generalization of eqn. (14) to mixtures which includes the addition of quantum corrections to the equation has been proposed.<sup>8</sup> Such modification has not improved the results.

### 3 Determination of EOS parameters for the system

#### 3.1 HSA parameters

The HSA model requires only one HS diameter for the  $N_2O_4$ – $NO_2$  system. The other HS diameter is calculated using the equation.

$$d_2/d_1 = 0.7784 \quad (23)$$

The approximation introduced in eqn. (23) comes from isothermal–isobaric Monte Carlo (MC) simulations<sup>9</sup> of fused hard sphere systems with atomic sizes and bond angles specified in Table 1, representing neat  $N_2O_4$  and neat  $NO_2$  fluids. The simulations were performed with 500-molecule systems with periodic boundary conditions. In the simulations, every cycle contained one movement attempt for each molecule and one volume change attempt. The MC results are averages of about 5000 equilibrated configurations, recorded every ten cycles. For  $N_2O_4$ , an average density of  $2.091 \text{ nm}^{-3}$  corresponded to a compressibility factor of 1.914, whereas for  $NO_2$  a density of  $4.283 \text{ nm}^{-3}$  corresponded to a compressibility factor of 1.869. For a pure HS system with properties described by the Carnahan–Starling EOS,<sup>10</sup> these MC results lead to a HS diameter of  $5.168 \text{ \AA}$  for  $N_2O_4$  and  $4.023 \text{ \AA}$  for  $NO_2$ ; eqn. (23) describes the ratio of such diameters. Alternatives to the approach described above would be, for instance, to determine the ratio of fused HS volumes or of excluded volumes (in the latter case, by the second virial coefficients). The cube roots of such ratios, 0.811 and 0.779 respectively, are in good agreement with eqn. (23) and yield virtually identical results.

HSA parameters were fitted to a state within the liquid–vapor coexistence region with pressure  $p = 1.1189 \text{ bar}$ ,<sup>11</sup>

**Table 1** Atomic diameters and structural data used for estimating the ratio of  $N_2O_4$  to  $NO_2$  HS diameters,  $d_1/d_2$  in the HSA model, and for estimating  $b_1/b_2$  ratios in the semiempirical EOS, eqn. (14) (see text)

Oxygen atom diameter <sup>a</sup>	3.04 $\text{\AA}$
Nitrogen atom diameter <sup>a</sup>	3.10 $\text{\AA}$
Chlorine atom diameter <sup>a</sup>	3.50 $\text{\AA}$
Carbon atom diameter <sup>a</sup>	3.40 $\text{\AA}$
Hydrogen atom diameter <sup>a</sup>	2.40 $\text{\AA}$
N–O internuclear distance ( $NO_2$ ) <sup>b</sup>	1.194 $\text{\AA}$
N–O internuclear distance ( $N_2O_4$ ) <sup>b</sup>	1.782 $\text{\AA}$
C–Cl internuclear distance ( $CCl_4$ ) <sup>c</sup>	1.766 $\text{\AA}$
C–C internuclear distance (cyclohexane) <sup>c</sup>	1.535 $\text{\AA}$
C–H internuclear distance (cyclohexane) <sup>c</sup>	1.092 $\text{\AA}$
O–N–O angle ( $NO_2$ ) <sup>b</sup>	133.8°
O–N–O angle ( $N_2O_4$ ) <sup>b</sup>	135.4°

<sup>a</sup> Ref. 29. <sup>b</sup> Ref. 30. <sup>c</sup> Ref. 17.

$D_L = 1.4357 \text{ g cm}^{-3}$  (liquid density) and  $\chi_2^L = 0.001668$  (mol fraction of  $NO_2$  in the liquid phase).<sup>11,12</sup>

Other authors have measured the equilibrium constant for the reaction in liquid  $N_2O_4$ ,<sup>13,14</sup> but the value used in this work (obtained by electron paramagnetic resonance EPR<sup>12</sup>) has been found to be consistent with corrected spectrophotometric data.<sup>15</sup> In addition, the EPR measurements were made at temperatures from 246.7 up to 296 K. Thus they can be used to test the model predictions for the liquid phase at other temperatures.

The set of parameters which satisfy the thermodynamical constraints referred to in Section 2.1 was optimized using Broyden's multidimensional secant method.<sup>16</sup> The following solution is obtained:  $d_1 = 4.485 \text{ \AA}$ ,  $a_1 = 2.848 \text{ J m}^3 \text{ mol}^{-2}$ ,  $a_2 = 0.557 \text{ J m}^3 \text{ mol}^{-2}$ .

HSA parameters for the neat solvent are needed for the calculation of properties of  $N_2O_4$  in equilibrium with  $NO_2$  in solution,  $d_3$  and  $a_3$ . These are chosen so as to yield the experimentally measured liquid density and vapor pressure at 298 K,<sup>17</sup> using the HSA equation of state. For  $CCl_4$  the parameters are  $d_3 = 5.260 \text{ \AA}$  and  $a_3 = 5.216 \text{ J m}^3 \text{ mol}^{-2}$ . For cyclohexane the parameters are  $d_3 = 5.466 \text{ \AA}$  and  $a_3 = 5.867 \text{ J m}^3 \text{ mol}^{-2}$ .

#### 3.2 SES parameters

The semiempirical EOS [eqn. (14)] requires for the  $N_2O_4$ – $NO_2$  system at least six parameters, three for each species, with the simplifications adopted for the mixture as described above. We have found that attempting to determine all parameters at once from a given set of experimental data often results in physically unreasonable parameters. For instance, negative parameter values or a  $N_2O_4$  HS diameter smaller than that for  $NO_2$ . To maintain consistency with the approaches adopted for the HSA model in this study, we again used MC simulations of neat fused HS systems. We should mention that, although both  $d_2/d_1$  and the  $c$  parameters could be determined by criteria based exclusively on body geometries and low density behavior, the semiempirical EOS formulation is set for better agreement with experimental data in the vicinity of the critical point. This feature leads to low-density data deviations, which implies that it is more adequate to run MC simulations to determine the SES parameters. However, we have evaluated the effect of using the low density approach. The overall agreement is similar, with better or worse prediction of the critical point density and temperature, depending on the assumptions made. The process for the semiempirical EOS parameter determination adopted in this work requires, in addition to the MC results listed in the previous section, two other runs. For  $N_2O_4$ , an average density of  $6.008 \text{ nm}^{-3}$  corresponded to a compressibility factor of 7.491, whereas in for  $NO_2$  a density of  $12.26 \text{ nm}^{-3}$  corresponded to a compressibility factor of 7.339. With the combined results, using the anisotropy-modified expression for Mansoori *et al.*'s EOS<sup>6</sup> for a pure HS fluid (equivalent to the Carnahan–Starling EOS<sup>10</sup>), the compressibility factor is

$$Z_{HS}^{anis.} = 1 + c \left[ \frac{4\eta - 2\eta^2}{(1 - \eta)^3} \right] \quad (24)$$

For  $N_2O_4$  one finds a HS diameter of  $4.995 \text{ \AA}$  and  $c = 1.157$ . For  $NO_2$ , the HS diameter is  $3.968 \text{ \AA}$  and  $c = 1.061$ . With such results, we set

$$d_2/d_1 = 3.968 \text{ \AA} / 4.995 \text{ \AA} = 0.7944 \quad (25)$$

The HS diameter ratio above is also consistent with both volume and excluded volume calculations (see Section 3.1).

Using the approximations above and the same experimental data used to fit the HSA parameters, one obtains the results listed in Table 2 for  $N_2O_4$  and  $NO_2$ .

**Table 2** Parameters  $T_i^*$ ,  $d_i$  and  $c_i$  for the semiempirical EOS [eqn. (14)] used in the calculations

Species $i$	$T_i^*/\text{K}$	$d_i/\text{\AA}$	$c_i$
$\text{N}_2\text{O}_4$	486.08	4.464	1.157
$\text{NO}_2$	168.14	3.546	1.061
$\text{CCl}_4$	524.91	5.197	0.1384
Cyclohexane	541.31	5.401	1.1557

The SES parameters for the solvent ( $\text{CCl}_4$  or cyclohexane) in eqn. (14) were chosen so as to yield the experimentally measured liquid density and vapor pressure at 298 K,<sup>17</sup> as adopted for the HSA model. In addition, the critical point (treated as a simple  $pVT$  point) was also taken as input because eqn. (14) requires three adjustable parameters for a neat fluid. Table 2 also lists the parameters for  $\text{CCl}_4$  and cyclohexane using the SES formulation.

## 4 Predictions and comparison with experimental data

### 4.1 Experimental data used for comparison with the model

Density measurements in the liquid–vapor coexistence region were taken from the work of Reamer and Sage.<sup>11</sup> Additional low temperature liquid density data were taken from another source.<sup>18</sup> Reamer and Sage's work also provided the pressure dependence of the liquid density at selected temperatures in the one-phase region.

The following gas experimental data were used. Pressure dependent gas phase mol fractions of  $\text{NO}_2$  at selected temperatures were from Yoshino *et al.*<sup>19</sup> Verhoek and Daniels<sup>20</sup> have given the density dependence of the equilibrium constant at selected temperatures.

Table 3 lists the  $\text{NO}_2$  mole fraction in the liquid phase,  $x_2^L$ , from experimental measurements<sup>12</sup> used for comparison with the model predictions. In the calculations, liquid density measurements mentioned above were used.<sup>11,18</sup>

Finally, Redmond and Wayland<sup>21</sup> have provided equilibrium constant data for the nitrogen oxides dissolved in organic solvents as a function of temperature and fraction of nitrogen oxides.

### 4.2 Model predictions and comparison with experimental data

**4.2.1  $\text{NO}_2$ – $\text{N}_2\text{O}_4$  system.** In all calculations, the thermodynamic values given by thermodynamic tables<sup>22</sup> for the ideal gas reference state were used.

The experimental and theoretical phase diagrams for the  $\text{NO}_2$ – $\text{N}_2\text{O}_4$  reacting system are shown in Fig. 1 (density–temperature) and Fig. 2 (pressure–temperature). The critical temperature predicted by the SES formulation [eqn. (14)] is in good agreement with the experimental value. The correspond-

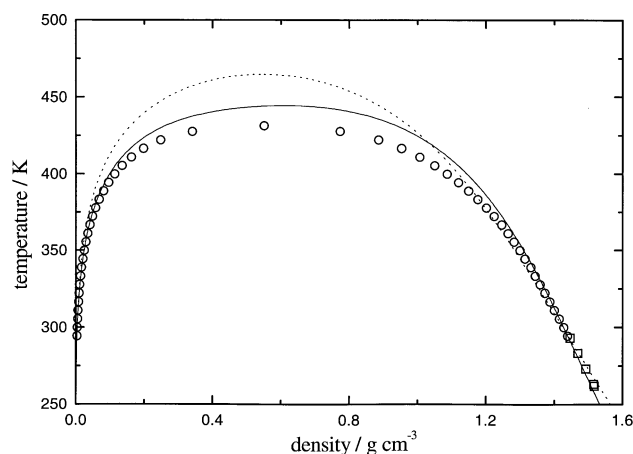


**Fig. 1** Temperature dependence of density in the liquid–vapor coexistence region of the  $\text{N}_2\text{O}_4$ – $\text{NO}_2$  reaction system. The theoretical HSA prediction is represented by the dotted line (---) and the semiempirical EOS [eqn. (4)] prediction by the solid line (—). The experimental points are represented by open squares ( $\square$ )<sup>18</sup> and open circles ( $\circ$ ).<sup>11</sup>

ing HSA prediction, somewhat less accurate, is about 5% higher than the SES prediction.

The agreement of both models with experimental phase equilibrium data is good, with a better performance for eqn. (14). However, it is necessary to acknowledge the fact that at  $T$  above 395 K the  $\text{N}_2\text{O}_4$  molecule starts to decompose, yielding  $\text{NO}$ ,<sup>23,24</sup> and that the higher the temperature the higher the amount of the  $\text{N}_2\text{O}_4$  isomer,  $\text{O}_2\text{N-O-NO}$  (0.32% at 373 K).<sup>15</sup> However, such side reactions do not significantly contribute to the observed phase diagram below 395 K. Tables 4 and 5 list calculated densities and  $\text{NO}_2$  mol fractions of the vapor and liquid phases in the coexistence region using the HSA and SES equations of state, respectively.

A comparison between the chemical equilibrium predictions in the liquid–vapor region using the HSA and SES approaches, along with purely ideal gas calculations (taking the calculated liquid and vapor densities from HSA), is made in Fig. 3. In Fig. 3, the mole fraction of  $\text{NO}_2$ ,  $x_2$ , is plotted as a function of temperature in the liquid–vapor region. The shape of all curves is very similar. The effect of non-ideality is of course evident in the liquid phase, where it contributes to a lower mole fraction of  $\text{NO}_2$  than what would be expected from purely ideal calculations. Although both models agree with each other around 296 K, they deviate significantly at higher temperatures. The better agreement of the SES prediction in Figs. 1 and 2 suggests that in Fig. 3 it may be the most accurate. Unfortunately, to the best of our knowledge there are no experimentally measured  $\text{NO}_2$  fraction data available above 300 K. According to the theoretical predictions, the maximum mole fraction of one of the species in the mixture is not achieved at the critical temperature. This is explained by the fact that high temperature favors  $\text{NO}_2$  (from the non-

**Table 3** Experimental mole fraction of  $\text{NO}_2$  in the liquid phase,  $x_2^L$  and  $\Delta G^{\text{rxn}} = -RT \ln K_c$  ( $\text{kJ mol}^{-1}$ ) in the liquid phase, where the equilibrium constant for the  $\text{N}_2\text{O}_4$  dissociation,  $K_c$ , is expressed in  $\text{mol dm}^{-3}$ ; the mole fraction of  $\text{NO}_2$  in the liquid phase,  $x_2^L$ , is calculated from equilibrium constants listed in ref. 12 and liquid density measurements from refs. 11 and 18

Temperature/K	$D_L/\text{g dm}^{-3}$	$x_2^L$	$\Delta G^{\text{rxn}} = -RT \ln K_c/\text{kJ mol}^{-1}$
246.65	<sup>a</sup>	—	32.86
256.35	<sup>a</sup>	—	30.40
266.05	1508.2	0.000 368 0	28.80
275.75	1485.9	0.000 563 4	27.93
286.45	1461.3	0.000 917 9	26.72
295.95	1435.7	0.001 668	24.71

<sup>a</sup> Liquid density data not available (thus  $x_2^L$  cannot be calculated from the data).

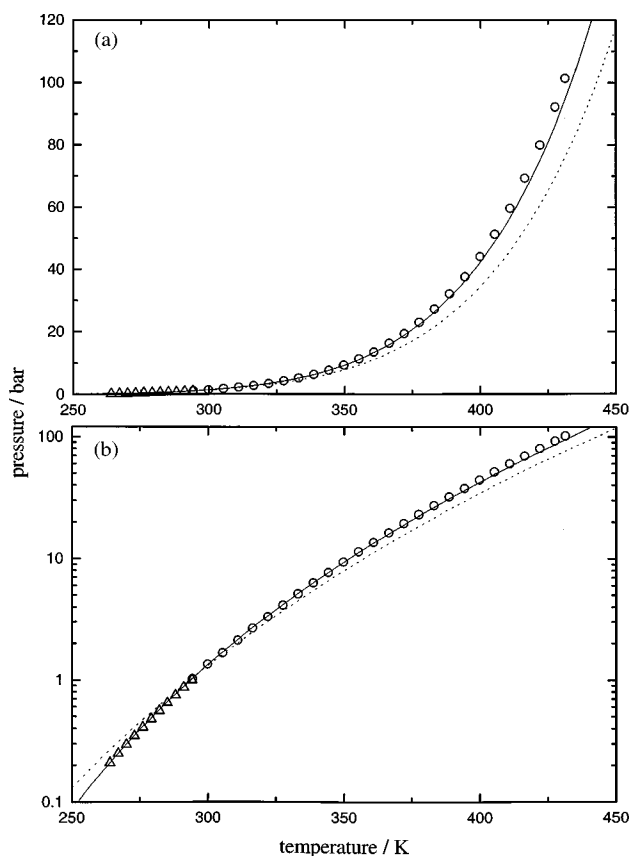


**Fig. 2** Temperature dependence of pressure in the liquid-vapor coexistence region of the  $\text{N}_2\text{O}_4$ - $\text{NO}_2$  reaction system. For better comparison, the same data are presented with the pressure in linear (a) and logarithmic (b) scales. The theoretical HSA prediction is represented by the dotted line (----) and the SES [eqn. (14)] prediction by the solid line (—). The experimental points are represented by open circles (○)<sup>11</sup> and open triangles (△).<sup>31</sup>

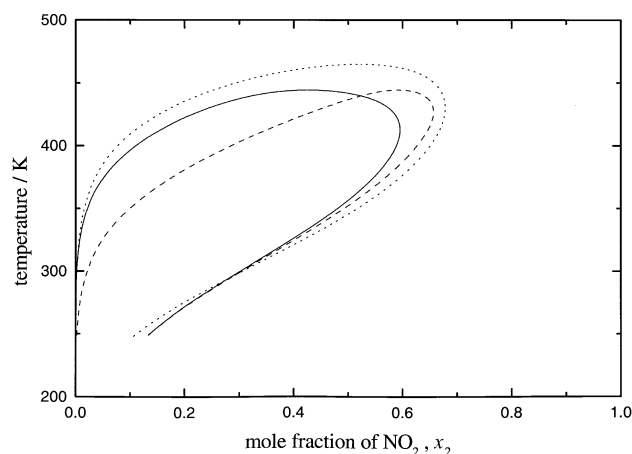


**Fig. 3** Temperature dependence of the mole fraction of  $\text{NO}_2$  in a  $\text{N}_2\text{O}_4$ - $\text{NO}_2$  reaction mixture in the liquid-vapor coexistence region. The dotted line (----) is predicted by the HSA model whereas the SES [eqn. (14)] prediction is indicated by the solid line (—). The dashed line (---) indicates the expected result if ideality is assumed and the densities from the SES calculations are taken.

interacting, ideal part of the free energy change upon reaction) whereas high pressure favors  $\text{N}_2\text{O}_4$  (because of the stoichiometric  $\text{N}_2\text{O}_4 : \text{NO}_2$  ratio). The balance between those two forces results in the observed feature in Fig. 3.

The pressure (or density) effect on the gaseous  $\text{NO}_2$ - $\text{N}_2\text{O}_4$  mixture at 298.5 K is shown in Fig. 4. The solid line indicates the prediction from ideal gas calculations, which is virtually indistinguishable from those using the HSA model and eqn. (14) in this pressure range. However, Table 6 shows the calculated  $(\partial K_p / \partial C_1^\circ)$  values at about 1 bar of the gas mixture (where  $K_p$  is the equilibrium constant for the dissociation of  $\text{N}_2\text{O}_4$ ) for each model along with the experimental measurements of Verhoek and Daniels.<sup>21</sup> The quantity  $C_1^\circ$  is the

**Table 4** Calculated densities ( $D$ ) and  $\text{NO}_2$  mole fractions ( $x_2$ ) of the vapor (V) and liquid (L) phases in the coexistence region using the HSA model

$T/\text{K}$	$p/\text{bar}$	Vapor phase		Liquid phase	
		$x_2^{\text{V}}$	$D_{\text{V}}/\text{g dm}^{-3}$	$x_2^{\text{L}}$	$D_{\text{L}}/\text{g dm}^{-3}$
250	0.13	0.112	0.55	0.000 12	1564
275	0.45	0.200	1.65	0.000 55	1494
300	1.32	0.307	4.18	0.002 03	1424
325	3.39	0.418	9.41	0.006 12	1355
350	7.93	0.517	19.5	0.015 9	1283
375	17.1	0.596	38.3	0.036 7	1207
400	34.4	0.651	72.5	0.077 3	1119
425	65.3	0.677	135.8	0.152	1009
450	117.8	0.658	267.3	0.294	839.1
464.8	163.6	0.524	540.9	0.524	540.9

**Table 5** Calculated densities ( $D$ ) and  $\text{NO}_2$  mole fractions ( $x_2$ ) of the vapor (V) and liquid (L) phases in the coexistence region using the SES formulation [eqn. (14)]

$T/\text{K}$	$p/\text{bar}$	Vapor phase		Liquid phase	
		$x_2^{\text{V}}$	$D_{\text{V}}/\text{g dm}^{-3}$	$x_2^{\text{L}}$	$D_{\text{L}}/\text{g dm}^{-3}$
250	0.086	0.136	0.36	0.000 057	1533
275	0.39	0.212	1.43	0.000 43	1480
300	1.35	0.302	4.30	0.002 11	1427
325	3.80	0.396	10.78	0.007 57	1371
350	9.35	0.481	24.0	0.021 7	1310
375	20.7	0.548	49.6	0.052 5	1238
400	42.3	0.589	99.1	0.111	1144
425	80.9	0.586	207.6	0.214	996.8
444.4	130.7	0.425	611.0	0.425	611.0

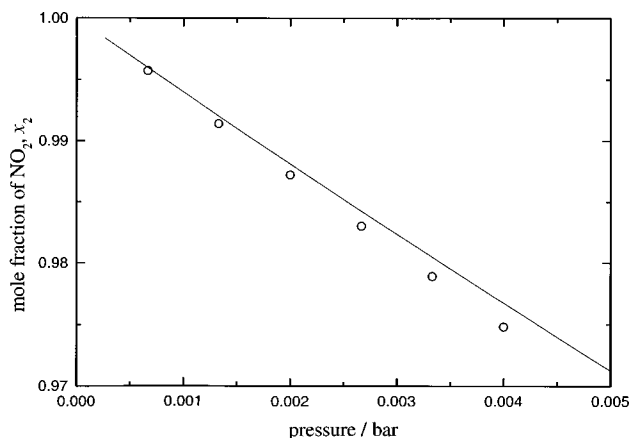


**Fig. 4** Comparison between experimental and theoretical mol fraction of  $\text{NO}_2$  in the vapor phase in a  $\text{N}_2\text{O}_4$ - $\text{NO}_2$  reaction mixture at 298.5 K. The experimental measurements (O) are taken from Yoshino *et al.*<sup>19</sup> and the theoretical predictions from ideal gas calculations are represented by the solid line (—). Such predictions are indistinguishable from those using the HSA model or eqn. (14).

density expressed as

$$C_1^\circ = \frac{m}{VM_1} \quad (26)$$

where  $m/V$  is the gas density in  $\text{g dm}^{-3}$  and  $M_1$  is the molecular weight of  $\text{N}_2\text{O}_4$ . The correct sign of  $\partial K_p/\partial C_1^\circ$  is predicted by both models. The discrepancy between experimental data and model predictions is expected for the HSA model, which has a mean field attractive term. The SES results [eqn. (14)] are somewhat closer to the experimental data, indicating that a temperature-dependent attraction is an improvement at such low pressures, although not sufficient.

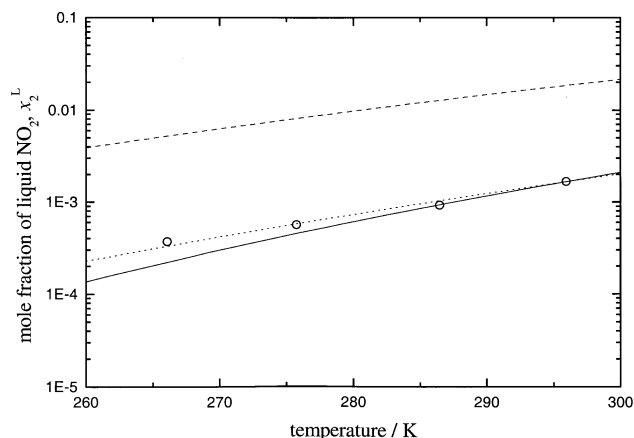
Good agreement between experimental data for  $x_2^L$  and the Gibbs free energy of reaction  $\Delta G^{\text{rxn}}$  (as defined in the figure caption) at  $T < 293$  K is obtained with the two models, as shown in Figs. 5 and 6. In the figures, results from ideal gas calculations at the same experimental liquid density are indicated as stars. Comparison between ideal gas and HSA results indicate that the non-ideality contributes most to the final result.

Table 7 lists HSA predictions of the liquid density as a function of pressure at 294.3 and 360.9 K and Table 8 lists the corresponding SES results. A comparison with experimental data is shown in Fig. 7. The SES results are in excellent agreement with the experimental data at 294.3 K, whereas the HSA predictions are more accurate at 360.9 K. Both approaches have a relatively similar overall accuracy, which is quite good, considering that only experimental data at 296 K in the liquid-vapor coexistence region were used to set the adjustable parameters.

#### 4.2.2 $\text{NO}_2$ - $\text{N}_2\text{O}_4$ in carbon tetrachloride and in cyclohexane. Table 9 compares the theoretical predictions of the dissociation constant of $\text{N}_2\text{O}_4$ , $\alpha$ , in $\text{CCl}_4$ with the experimen-

**Table 6** Comparison between experimental<sup>20</sup>  $\partial K_p/\partial C_1^\circ$ , as defined in eqn. (23), and theoretical predictions (HSA and SES) at 0.5–1 bar (gas phase)

Method	$\partial K_p/\partial C_1^\circ$		
	298 K	308 K	318 K
Experimental	-0.769	-1.612	-3.427
HSA	-0.096	-0.185	-0.338
SES	-0.151	-0.273	-0.475



**Fig. 5** Temperature dependence of the mol fraction of  $\text{NO}_2$  in the liquid phase,  $x_2^L$ , in a  $\text{N}_2\text{O}_4$ - $\text{NO}_2$  reaction mixture. Experimental results (O) are taken from Table 3 whereas HSA predictions are represented by the dotted line (----) and SES [eqn. (4)] predictions by the solid line (—). Ideal gas calculations, obtained for the same experimental liquid density, are represented by the dashed line (---) and clearly indicate the importance of accounting for the non-ideality of the system.

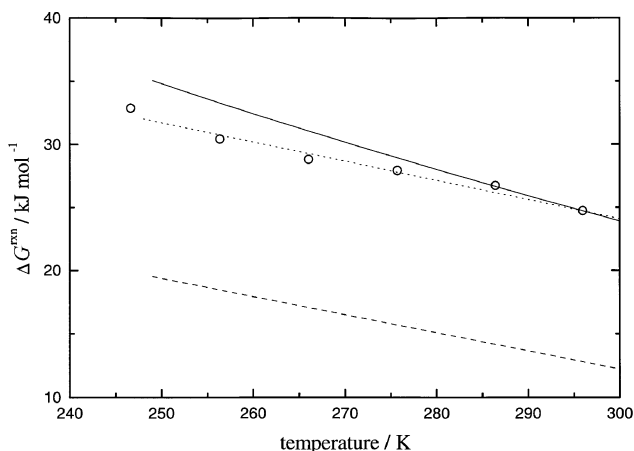


**Fig. 6** Temperature dependence of  $\Delta G^{\text{rxn}} = -RT \ln K_c$  (in  $\text{kJ mol}^{-1}$ ) in the liquid phase, where the equilibrium constant  $K_c$  is expressed in  $\text{mol dm}^{-3}$ , in a  $\text{N}_2\text{O}_4$ - $\text{NO}_2$  reaction mixture. Experimental results (O) are taken from Table 3 whereas HSA predictions are represented by the dotted line (----) and SES predictions by the solid line (—). Ideal gas calculations, obtained for the same experimental liquid density, are represented by the dashed line (---) and clearly indicate the importance of accounting for the non-ideality of the system.

**Table 7** HSA predictions of the liquid density ( $D$ ) and mole fraction of  $\text{NO}_2$ ,  $x_2$ , as a function of pressure at 294.3 and 360.9 K in the one-phase region

T/K	EOS predictions		
	$x_2$	$D/\text{g dm}^{-3}$	$p/\text{bar}$
294.3	0.001 52	1443	12.3
294.3	0.001 45	1461	94.5
294.3	0.001 36	1481	194.6
294.3	0.001 29	1501	304.9
294.3	0.001 25	1511	364.1
360.9	0.0234	1248	4.0
360.9	0.0217	1278	85.8
360.9	0.0202	1308	181.5
360.9	0.0187	1338	292.9
360.9	0.0174	1368	421.6

**Table 8** SES predictions [eqn. (14)] of the liquid density  $D$  and mole fraction of  $\text{NO}_2$ ,  $x_2$  as a function of pressure at 294.3 and 360.9 K in the one-phase region

$T/\text{K}$	SES predictions		
	$x_2$	$D/\text{g dm}^{-3}$	$p/\text{bar}$
294.3	0.001 51	1440	5.15
294.3	0.001 40	1460	130.4
294.3	0.001 31	1480	270.1
294.3	0.001 21	1500	425.3
360.9	0.0326	1280	11.3
360.9	0.0311	1300	76.0
360.9	0.0296	1320	150.1
360.9	0.0282	1340	234.1
360.9	0.0268	1360	328.8
360.9	0.0254	1380	435.1

tal values from Redmond and Wayland<sup>21</sup> as a function of temperature and mass fraction of the nitrogen oxides ( $\text{N}_2\text{O}_4 + \text{NO}_2$ ) in the solution. HSA calculations for  $\text{N}_2\text{O}_4\text{-NO}_2$  dissolved in organic solvents indicate a reasonably good agree-

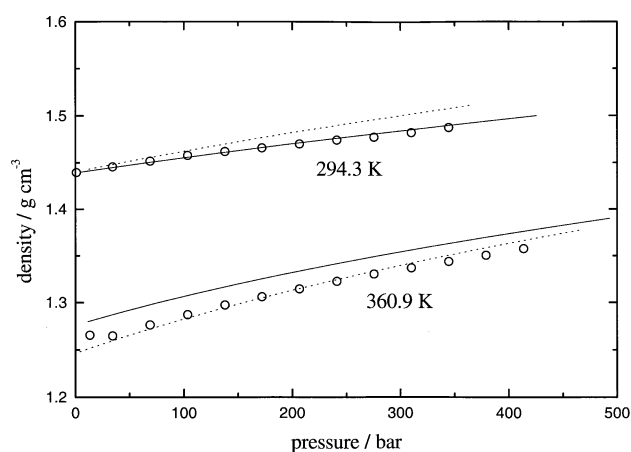


**Fig. 7** Pressure dependence of  $\text{N}_2\text{O}_4$  at selected temperatures. The dotted lines (----) are HSA predictions, the solid lines (—) are SES predictions, and the open circles (O) represent experimental measurements by Reamer and Sage.<sup>11</sup>

**Table 9** Comparison between experimental measurements<sup>21</sup> and theoretical (HSA and SES) predictions of  $\text{N}_2\text{O}_4$  dissociation constants ( $\alpha$ ) for the system  $\text{N}_2\text{O}_4\text{-NO}_2\text{-CCl}_4$ ; the quantity  $x_m$  is the mass fraction of the nitrogen oxides in the solution

$T/\text{K}$	$x_m$	$\alpha$		
		Experimental	HSA	SES
299.7	0.0695	0.0065	0.0041	0.0046
308.2	0.0412	0.0117	0.0079	0.0096
308.5	0.0695	0.0094	0.0061	0.0075
323.2	0.0695	0.0158	0.0113	0.0155
326.2	0.0412	0.0241	0.0166	0.0230

**Table 10** Comparison between experimental measurements<sup>21</sup> and theoretical (HSA and SES) predictions of  $\text{N}_2\text{O}_4$  dissociation constants ( $\alpha$ ) for the system  $\text{N}_2\text{O}_4\text{-NO}_2\text{-cyclohexane}$ ; the quantity  $x_m$ , defined in the text, is the mass fraction of the nitrogen oxides in the solution

$T/\text{K}$	$x_m$	$\alpha$		
		Experimental	HSA	SES
299.9	0.0959	0.0072	0.0054	0.0075
299.9	0.123	0.0066	0.0048	0.0065
307.5	0.0958	0.0098	0.0076	0.0113
307.5	0.123	0.0088	0.0067	0.0098
315.2	0.0957	0.0141	0.0106	0.0166
315.2	0.123	0.0123	0.0093	0.0145
323.2	0.0956	0.0183	0.0146	0.0242
323.2	0.123	0.0164	0.0128	0.0211

ment with experimental data. They underestimate the dissociation constant of  $\text{N}_2\text{O}_4$  in the liquid phase by about 30%. The systematic deviation when eqn. (14) is used is about 15%.

Similar results are obtained by comparing the model predictions of the dissociation constant of  $\text{N}_2\text{O}_4$  in cyclohexane (Table 10). The calculated HSA values are about 25% smaller than the experimentally measured values whereas the SES results [eqn. (14)] are about 15% greater.

## 5 Discussion and conclusions

The results of this work show how well simple approximations about the nature of the interactions between the molecules in the  $\text{N}_2\text{O}_4\text{-NO}_2$  system, with and without solvent, can be used to produce fairly accurate predictions of the phase behavior,  $pVT$  properties in general and equilibrium constant. For one-phase systems, great improvements are obtained simply by accounting for the non-ideality of the system with a simple model such as HSA. Given few experimental data, it is possible to obtain reasonably accurate interpolations and predictions in the vicinity of the gathered data.

The results obtained in this paper suggest that the simple HSA EOS, which models all species as hard spheres with mean field attractive parameters, is one approach (among several similar ones) which can be applied to obtain reasonable estimates of equilibrium constants as well as phase equilibria and  $pVT$  data. Such relatively good results can be obtained with few experimental data as inputs. Depending on the cost involved in making accurate experimental measurements and the required accuracy and reliability of the property of interest, the HSA model could be a very useful approach, especially when very few (yet representative) experimental data are available.

For the  $\text{N}_2\text{O}_4\text{-NO}_2$  system, the semiempirical EOS given by eqn. (14) has the flexibility to successfully fit a greater number of representative data points, with a clear increase in accuracy compared to the HSA EOS. Such an approach may be more appropriate when more experimental data are available because it has more realistic features than the HSA EOS. For example, it accounts for the anisotropy of the molecules and contains a temperature-dependent attractive term. However, one must be very careful when applying eqn. (14) to

reacting systems when few experimental data are available. Sets of parameters with physically meaningless values, which cannot be used to predict outside the range of experimental data, may be obtained. An additional problem is that one must also have a good knowledge of what range of values for each parameter is acceptable. Finally, the number of parameters may need to be reduced if little experimentally relevant information is available. In this work, the approach of getting reasonable values for the anisotropy parameters  $c$  from MC simulations was very successful. In general, for good strategies, physically sound algorithms are required. We have also tested the performance of the simplified perturbed hard chain theory (SPHCT)<sup>25,26</sup> for the  $\text{N}_2\text{O}_4\text{-NO}_2$  system, adopting three adjustable parameters per species by making similar simplifications to those used in the HSA model. The SPHCT results were somewhere between the HSA and SES [eqn. (14)] ones. However, we faced the same problems during the fitting procedure as those described above when eqn. (14) was used, indicating that such problems may be common when using more accurate (with more adjustable parameters than HSA) equations of state. It should be noted that in both SES and SPHCT cases, simply increasing the number of adjustable parameters with simultaneous use of more experimental data did not result in any reduction of deviations from experimental measurements and at the same time the difficulty in fitting increased.

The SES results of the  $\text{N}_2\text{O}_4$  dissociation constant in organic solvents are clearly more accurate than those using the HSA model. For such a system, the choice of mixing rules becomes more important because no experimental data for the ternary system were taken as input in the fitting procedure. We believe that, when extending the use of the eqn. (14) to more complex mixtures, the choice of mixing rules becomes more important. The systematic deviation of results (although small) for  $\text{N}_2\text{O}_4\text{-NO}_2$  in organic solvents using eqn. (14) suggests the importance of taking representative experimental points to adjust the mixing rules.

Modern equations of state are most commonly applied and tested against  $pVT$  properties and phase equilibria. Computer simulations have the advantage of being able to take molecular shape into account very easily whereas equations of state can rarely do better than using a single shape parameter. However, equations of state parameters can be determined with great ease from experimental data whereas simulations require several runs and more computer time. In some cases, such as the  $\text{N}_2\text{O}_4\text{-NO}_2$  system, MC simulations would require applying the computationally costly two-phase reactive ensemble method<sup>27,28</sup> because  $\text{N}_2\text{O}_4$  and  $\text{NO}_2$  are in equilibrium and relevant experimental data for setting the parameters involve two phases with significant amounts of both species. In addition, the interaction potential would probably require atom-atom potentials with the use of partial charges. Because virtually all experimental data are incomplete (for example, density and temperature are given, but not composition), a great number of simulations would be required at different pressure and temperature values. Such simulations would be then repeated several times with different interaction parameters until the observed properties were reproduced.

When equations of state are tested, much insight may be gained if the properties of reacting systems are also included.

This would also require an effort to obtain more experimental data, containing  $pVT$  properties along with equilibrium constants over a wide range of pressure and temperature. In this work, the composition of each phase of the  $\text{N}_2\text{O}_4\text{-NO}_2$  system in the liquid-vapor coexistence region above 300 K was included so that in the future, perhaps, the accuracy of the models presented here can be evaluated in more detail.

## Acknowledgements

L. de Souza was fully supported by a postdoctoral fellowship provided by the Alexander von Humboldt Foundation.

## References

- 1 L. E. S. de Souza and D. Ben-Amotz, *J. Chem. Phys.*, 1994, **101**, 4117.
- 2 R. Ravi, L. E. S. de Souza and D. Ben-Amotz, *J. Phys. Chem.*, 1993, **97**, 11835.
- 3 U. Deiters, *Chem. Eng. Sci.*, 1981, **36**, 1139.
- 4 U. Deiters, *Chem. Eng. Sci.*, 1981, **36**, 1147.
- 5 U. Deiters, *Chem. Eng. Sci.*, 1982, **37**, 855.
- 6 G. A. Mansoori, N. F. Carnahan, K. E. Starling and T. W. Leland, Jr., *J. Chem. Phys.*, 1971, **54**, 1523.
- 7 U. K. Deiters, *Fluid Phase Equilib.*, 1987, **33**, 267.
- 8 U. K. Deiters, M. Neichel and K. E. Frank, *Ber. Bunsen-Ges. Phys. Chem.*, 1993, **97**, 649.
- 9 M. P. Allen and D. J. Tildesley, in *Computer Simulation of Liquids*, Oxford University Press, New York, 1991, pp. 123–126.
- 10 N. F. Carnahan and K. E. Starling, *J. Chem. Phys.*, 1969, **51**, 635.
- 11 H. H. Reamer and B. H. Sage, *Ind. Eng. Chem.*, 1952, **44**, 185.
- 12 D. W. James and R. C. Marshall, *J. Phys. Chem.*, 1968, **72**, 2963.
- 13 C. M. Steese and A. Greenville Whittaker, *J. Chem. Phys.*, 1956, **24**, 776.
- 14 A. J. Vosper, *J. Chem. Soc. A*, 1970, 2191.
- 15 D. A. Pinnick, S. F. Agnew and B. I. Swanson, *J. Phys. Chem.*, 1992, **96**, 7092.
- 16 W. H. Press, S. A. Teukolsky, W. T. Vetterling and B. P. Flannery, in *Numerical Recipes*, 2nd edn., Cambridge University Press, New York, 1992, pp. 382–386.
- 17 *CRC Handbook of Chemistry and Physics*, 72nd edn., ed. David R. Lide, CRC Press, Boca Raton, FL, 1991.
- 18 P. Gray and P. Rathbone, *J. Chem. Soc.*, 1958, 3550.
- 19 K. Yoshino, J. R. Esmond and W. H. Parkinson, *Chem. Phys.*, 1997, **221**, 169.
- 20 F. H. Verhoek and F. Daniels, *J. Am. Chem. Soc.*, 1931, **53**, 1250.
- 21 T. F. Redmond and B. B. Wayland, *J. Phys. Chem.*, 1968, **72**, 1626.
- 22 *TRC Thermodynamic Tables—Non-Hydrocarbons*, ed. M. Frenkel, N. M. Gadalla, K. R. Hall, X. Hong, K. N. Marsh and R. C. Wilhoit, Thermodynamics Research Center, The Texas A&M University System, College Station, TX, 1997, pp. 470 and 471.
- 23 *Supplement to Mellor's Comprehensive Treatise on Inorganic and Theoretical Chemistry*, vol. VIII, suppl. II, Nitrogen (part II), Longmans, London, 1967.
- 24 Q. Yu and H. Gao, *J. Chem. Educ.*, 1997, **74**, 233.
- 25 M. D. Donohue and J. M. Prausnitz, *AIChE J.*, 1978, **24**, 849.
- 26 C. H. Kim, P. Vimalchand, M. D. Donohue and S. I. Sandler, *AIChE J.*, 1986, **32**, 1726.
- 27 W. R. Smith and B. Triska, *J. Chem. Phys.*, 1994, **100**, 3019.
- 28 L. E. S. de Souza and U. K. Deiter, *Phys. Chem. Chem. Phys.*, 1999, **1**, 4069.
- 29 A. Bondi, *J. Phys. Chem.*, 1964, **68**, 441.
- 30 A. Stirling, I. Pápai, J. Mink and D. R. Salahub, *J. Chem. Phys.*, 1994, **100**, 2910.
- 31 W. F. Giauque and J. D. Kemp, *J. Chem. Phys.*, 1938, **6**, 40.